esoc

European Space Operations Centre
Robert-Bosch-Strasse 5
D-64293 Darmstadt
Germany
T +49 (0)6151 900
F +49 (0)6151 90495
www.esa.int

DOCUMENT

EDRS-C/NGRM Level 1 data description

EDRS-C/NGRM Level 1 datasets

Prepared by **Ingmar Sandberg**
Space Applications & Research Consultancy

Reference **SPARC-EDRSC-NGRM-L1 Data Description**
Issue/Revision **1.0**
Date of Issue **28/02/2022**
Status **Released**

European Space Agency
Agence spatiale européenne

APPROVAL

Title EDRS-C/NGRM Level 1 datasets	
Issue Number 1	**Revision Number** 0
Author Ingmar Sandberg	**Date** 28/02/2022
Approved By	**Date of Approval**
Melanie Heil	Digitally signed by Melanie Heil Date: 2022.03.02 16:02:34 +01'00'

CHANGE LOG

Reason for change	Issue Nr.	Revision Number	Date

DISTRIBUTION

Name/Organisational Unit

Table of contents:

Table of figures:

Table of tables:

1 REFERENCE DOCUMENTS AND ACRONYMS

1.1 Reference Documents

[RD 1] L. Desorgher, W. Hajdas, I. Britvitch, K. Egli, X. Guo, Y. Luo, F. Chastellain, C. Pereira, R. Muff, D. Boscher, G. Maehlum, and D. Meier, “The next generation radiation monitor- NGRM,” in 2013 IEEE Nuclear Science Symposium and Medical Imaging Conference (2013 NSS/MIC). IEEE, Oct. 2013, pp. 1–6.

[RD 2] S. Agostinelli et al., “Geant4—a simulation toolkit,” Nuclear Instruments and Methods in Physics Research Section A: Accelerators, Spectrometers, Detectors and Associated Equipment, vol. 506, no. 3, pp. 250–303, Jul.2003.

[RD 3] I. Sandberg et al., "Data Exploitation of New Galileo Environmental Monitoring Units," in IEEE Transactions on Nuclear Science, vol. 66, no. 7, pp. 1761-1769, July 2019

[RD 4] S. Aminalragia-Giamini et al 2018, Artificial intelligence unfolding for space radiation monitor data, J. Space Weather Space Clim. 2018, 8, A50, https://doi.org/10.1051/swsc/2018041

[RD 5] A. Boudouridis, J. Rodriguez, B. Kress, B. Dichter, and T. Onsager, “Development of a bowtie inversion technique for real-time processing of the GOES-16/-17 SEISS MPS-HI electron channels,” Space Weather, vol. 18, no. 4, Apr. 2020.

[RD 6] SEPEM reference data set (rds) v2.X 2017a, http://test.sepem.eu/help/SEPEM RDS v2-00.zip

[RD 7] I. Sandberg, P. Jiggens, D. Heynderickx, and I. A. Daglis, “Cross calibration of NOAA GOES solar proton detectors using corrected NASA IMP-8/GME data”, Geophysical Research Letters, vol. 41, no. 3, pp. 4435- 4441, 2014d

[RD 8] Sandberg et al, “First results and analysis from ESA Next Generation Radiation Monitor unit on-board EDRS-C”, *Accepted for publication* in IEEE Transactions on Nuclear Science.

[RD 9] Higashio et al., The extremely high-energy electron experiment (XEP) onboard the Arase (ERG) satellite Earth, Planets and Space (2018) 70:134 https://doi.org/10.1186/s40623-018-0901-x]

[RD 10] UNILIB http://www.mag-unilib.eu/

1.2 Acronyms

Acronyms used in this document and needing a definition can be found in:

Acronym	Definition
AI	Artificial Intelligence
BT	Bow-Tie
CBR	Case-Based-Reasoning
EDRS-C	European Data Relay Satellite C
EMU	Environmental Monitoring Unit
ESA	European Space Agency
EDSS	Electron Detector Sub-System
ESOC	European Space Operations Centre
ESTEC	European Space Research and Technology Centre
HEO	Highly Elliptic orbit
GA	Genetic Algorithm
GenCORUM	Genetic Correlative Unfolding Method
GP	Ground Processor
GTO	Geostationary Transfer Orbit
FEDO	Omni-directional Differential Electron Flux
FEIO	Omni-directional Integral Electron Flux
FPDO	Omni-directional Differential Proton Flux
FPIO	Omni-directional Integral Proton Flux
MagEIS	Magnetic Electron Ion Spectrometer
NGRM	Next Generation Radiation Monitor
ODI	Open Data Interface
PODC	Payload Operation Data Centre
RB	Radiation Belts
RBSP	Radiation Belt Storm Probes
REPT	Relativistic Electron-Proton Telescopes
RF	Response Function
SDSS	Stacked Detector Sub-System
SEP	Solar Energetic Particle
TAS	Thales Alenia Space
TN	Technical Note
XEP	extremely high-energy electron experiment

Table 1: Acronyms

2 INTRODUCTION

2.1 Purpose

This document describes the main characteristics of the released EDRS-C NGRM Level 1 Version 3 datasets and highlights the methods used for their derivation.

2.2 Background

ESA Next Generation Radiation Monitor (NGRM) was designed to measure protons from 2 MeV up to 200 MeV, electrons from 100 keV up to 7 MeV. The first unit was placed on-board the Geostationary (GEO) European Data Relay System, Satellite-C (EDRS-C), launched on the 6th August 2019. NGRM development started within a consortium led by TAS-CH space (former RUAG space), together with Paul Scherrer Institute (PSI), Office National d'Etudes et de Recherches Aerospatiales (ONERA), EREMS, and Integrated Detector Electronics AS (IDEAS). Within "SSA P3-SWE-XXI NGRM Data Processing activity", SPARC led a consortium that included Solenix, SE2S and DHConsultancy, as external service provider, aiming to the design and the implementation of the NGRM Ground Processor. The performed developments included, among others, the derivation of the response functions for the NGRM unit on-board EDRS-C and the development and implementation of methods for the derivation of NGRM Level 1 flux products.

2.3 ESA NEXT GENERATION RADIATION MONITOR

The NGRM unit includes the electron and the stacked detector subsystems [RD 1] . The electron detector subsystem (EDSS) provides measurements in 16 channels while the stacked (proton) detector subsystem (SDSS) has 10 channels. EDSS is a circular strip detector made of 16 strips covered by a collimator made by an aluminium part on the bottom and covered by a copper cone on the top. The collimator is embedded in the aluminium housing acting as a field-of-view limiter and side shielding against particles coming from other directions. The aluminium part of the collimator is made by a concentric succession of 12 circular stairs with different thicknesses. Each silicon circular strip is bonded to an ASIC high gain channel where particles are counted when their deposited energy is within the range fixed by the low and high detection thresholds of the corresponding ASIC channel. SDSS consists of a stack of 7 Silicon cylindrical diodes separated by aluminium and tantalum degraders of different thicknesses. The diodes and the absorbers are shielded from the side by copper and aluminium cylinders. The aperture of the detector has a half opening angle of 40 degrees. Energetic particles coming from the top through the aperture cone are detected by ionization in a diode if they have sufficient minimum energy to cross all the previous degraders and diodes. The ionization current generated by a particle crossing the diode is processed by ASIC electronic circuits.

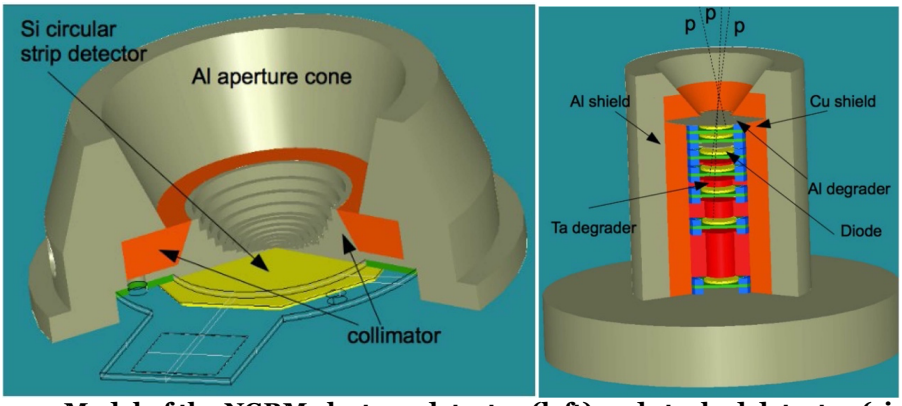

Figure 1: Model of the NGRM electron detector (left) and stacked detector (right).

3 CALIBRATION OF NGRM UNIT

The electron (proton) response functions (RF) of the EDSS (SDSS) of NGRM on-board EDRS-C have been derived on the basis of experimental and GEANT4 [RD 2] numerical calibrations. The response curves were numerically derived and then re-adjusted using the experimental results of the unit's experimental calibrations that took place at the Proton Irradiation and at the Electron Monochromator Facilities at Paul Scherrer Institute in Switzerland. The curves of the response functions that are used for the derivation of the EDRS-C/NGRM Level 1 flux products are presented below.

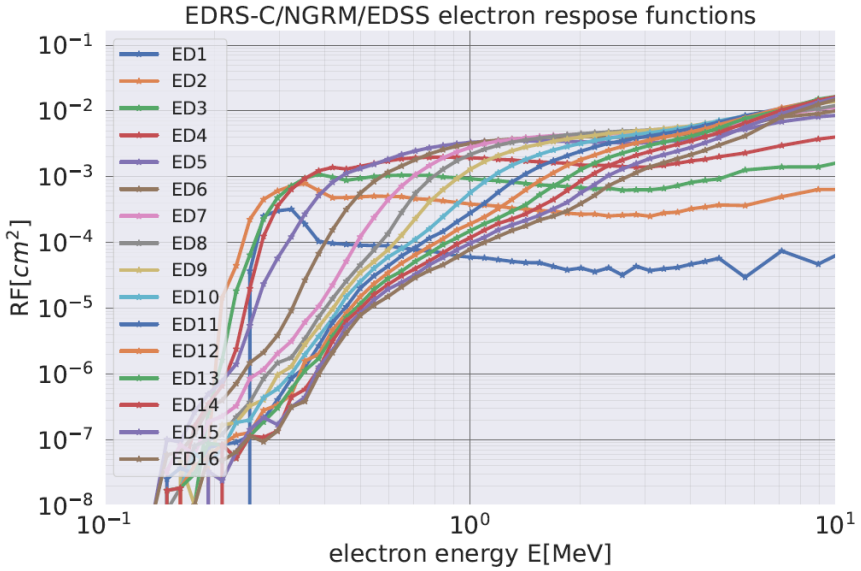

Figure 2: Omni-directional electron response functions of EDRS-C/NGRM Electron Detector (ED) channels.

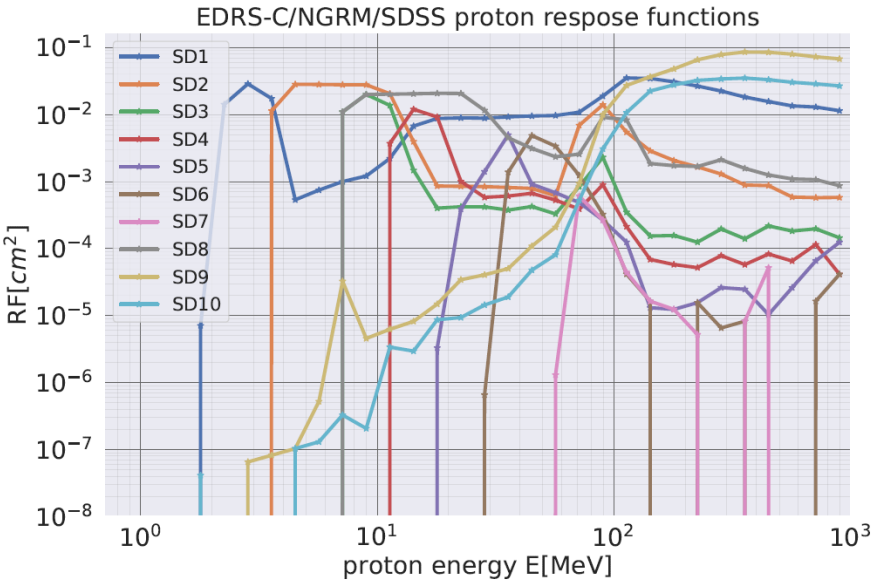

Figure 3: Omni-directional proton response function of EDRS-C/NGRM Stacked Detector (SD) channels.

4 DATA CALIBRATION

The conversion of count data to calibrated energetic particle fluxes, corresponds to the derivation of solutions of the one-dimensional unfolding problem where the response (measurements) *C* of a detector is the result of the convolution of the incident differential particle fluxes *f(E)* with the response function *RF(E)* of the unit.

$$C = \int_0^\infty f(E)\, RF(E)\, dE \qquad \textbf{Equation 1}$$

For the derivation of EDRS-C NGRM Level-1 fluxes two different methodologies were employed. For the calculation of proton differential fluxes and electron integral fluxes, single multiplicative scaling factors were derived and applied for each channel using the Bow-Tie (BT) analysis [RD 3]. The BT analysis allows the derivation of a scaling factor for the conversion of the detector's count rates to flux products for an energy value that minimizes the uncertainties expected at the encountered space radiation environment. For the calculation of electron differential fluxes, the Genetic Correlative Unfolding Method (GenCORUM) was applied. The GenCORUM [RD 4] is an artificial intelligence method which employs a Cased-Based Reasoning (CBR) process coupled with a Genetic Algorithm (GA).

4.1 Electron Integral Flux Dataset: Level 1 Version 3

For the calculation of electron integral fluxes, a data-driven variant [RD 3] of the commonly used Bow-Tie (BT) analysis approach was implemented. For the sampling of the electron radiation environment at GEO the differential electron flux measurements from the MPS-Hi [RD 5] unit on-board NOAA GOES-16 were used. This particular GEO electron differential flux dataset was selected due to its relative extensive energy range. The GEO MPS-Hi electron flux measurements were initially fitted, using a power law with an exponential cutoff, and the resulting dataset, i.e. *f (E,t)* was used for the derivation of suitable NGRM scaling factors following the procedure below.

For each ED channel, distributions of geometric factors $GF(E_i, t)$ for different energies E_i were derived through the integration of the training differential flux spectra with the corresponding response function divided by the training integral flux spectra:

$$GF(E_i, t) = \frac{\int_0^\infty RF(E)\, f(E) dE}{\int_{Ei}^\infty f(E) dE} \qquad \textbf{Equation 2}$$

A characteristic bow-tie energy was determined for each channel as the optimum value that minimizes the mean squared error of the distribution of the logarithmic values of the geometric factors. This approach was applied only for the first 10 out of 16 ED channels, as the bow-tie energy values of the last channels were very close to each other. This was an expected result due to the similar characteristics of the electron response curves of these channels. Thus, for the last 6 ED channels, the standard BT approach was discarded and the characteristic energies for these channels were pre-selected within the range of 1.6-2.2 MeV. This approach permitted the extension of the energy range of the derived integral flux spectra at the cost of increasing the uncertainties of the derived integral flux values for energies above 1.6 MeV. In all cases, the median value of the resulted distributions was selected for the definition of the scaling factor, i.e., $SF_{50}=1/median(GF(E_{BT}))$, for each channel.

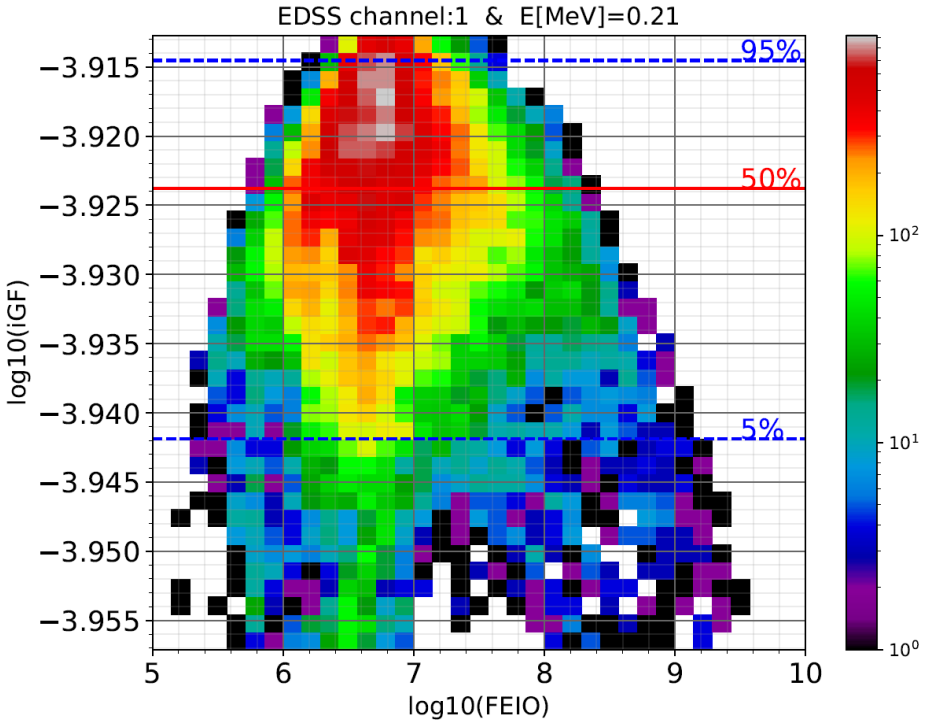

Figure 4: Histogram of the distribution of the geometric factors for the first channel at E=0.21 MeV, derived using Equation 1. The horizonal lines denote selected percentiles of the geometric factors.

For a quantitative evaluation of the uncertainties of the derived electron flux which are attributed to the selection of the median value of the distribution of the geometric factors - as derived by using as sample the GEO MPS-Hi dataset – we have calculated the uncertainties using the extremes in the sampled GEO electron radiation environment measurements.

The table below summarizes the analysis and the results associated to the derivation of the EDRS-C NGRM electron integral fluxes - which have been introduced in the Level 1 Version 3 NGRM dataset – and include also the relative differences between the 1% and the 99% percentiles of the scaling factor distributions with respect to the median value (50% percentile) which was used for the derivation of the integral electron fluxes.

Table 2: Characteristics of L1 V3 EDRS-C/NGRM electron integral flux dataset.

Flux Bin	EDSS channel	FEIO_ENERGY [MeV]	SF50	(SF1-SF50)/SF1	(SF99-SF50)/SF99
1	1	0.209	8390	0.074	-0.026
2	2	0.235	2018	0.034	-0.013
3	3	0.286	1070	0.009	-0.006
4	4	0.338	599	0.008	-0.018
5	5	0.455	376	0.024	-0.061
6	6	0.594	330	0.026	-0.077
7	7	0.736	294	0.027	-0.083
8	8	0.841	287	0.030	-0.092
9	9	0.944	319	0.040	-0.138
10	10	1.043	404	0.053	-0.185
11	11	1.2	410	0.092	-0.219
12	12	1.4	326	0.213	-0.374
13	13	1.6	257	0.341	-0.620
13	13	1.8	201	0.455	-0.929
15	15	2	158	0.557	-1.305
16	16	2.2	115	0.667	-1.806

The negative sign in the last column indicates an overestimation of the BT flux products with respect to the 0.99 percentile.

The calculation of the integral electron fluxes FEIO requires the application of the following scheme,

$$FEIO[FEIO_{ENERGY}] = \frac{SF_{50} \times ED_{COUNTRATE}}{4\pi} \; [cm^2 \sec str]^{-1} \qquad \textbf{Equation 3}$$

which takes place on-the-fly as soon as raw ED measurements become available at NGRM Ground Processor.

4.2 Proton Differential Flux Dataset: Level 1 Version 3

For the calculation of proton differential fluxes, a BT analysis of NGRM SDSS proton responses was applied using the Solar Energetic Particle Environment Modelling (SEPEM) reference dataset (SEPEM RDS) [RD 6] as a training dataset. SEPEM is based on NOAA GOES proton flux measurements cross-calibrated by [RD 7] using as reference the IMP-8 Goddard Medium Energy experiment.

The presence of strong cross-contamination effects in SD channels 1, 8, 9 and 10 currently does not allow the use of their measurements at GEO. In what follows we summarize the results of the BT analysis for SD channels 2-7 which provide the proton differential flux products in Level 1 dataset.

Table 3: Characteristics of EDRS-C/NGRM proton differential flux dataset.

Flux Bin	SD channels	FPDO Energy [MeV]	(SF1-SF50)/SF1	(SF99-SF50)/SF99
1	2	5.51	0.022	-0.15
2	3	8.80	0.0091	-0.061
3	4	14.83	0.0089	-0.067
4	5	33.92	0.010	-0.062
5	6	46.06	0.0098	-0.042
6	7	76.24	0.0061	-0.037

The calculation of the proton differential fluxes FPDO requires the application of the following scheme,

$$FPDO[FPDO_{ENERGY}] = \frac{SF_{50} \times SD_{COUNTRATE}}{4\pi} \; [cm^2 \sec str]^{-1} \qquad \textbf{Equation 4}$$

which takes place on-the-fly as soon as raw SD measurements become available at NGRM Ground Processor.

4.3 Electron Differential Flux Dataset: Level 1 Version 3

The application of any direct re-scaling approach results to uncertainties in the derivation of differential particle fluxes. This is especially true for energies above 1.5 MeV in the case of NGRM units where the electron response functions are of integral-type. Thus, for the derivation of the electron differential fluxes, the GenCORUM method was adopted. GenCORUM is an artificial intelligence method which combines two different methodologies; a Case-Based-Reasoning (CBR) process and a Genetic Algorithm (GA). The CBR process performs an initial "rough" unfolding producing particle spectra and this output is forwarded to the GA which fine-tunes each spectrum independently producing the final unfolded particle fluxes.
During the CBR process, a virtual "library" is created by folding virtual electron flux spectra derived from an exponential cut-off power-law function with ED electron response functions and producing the counterpart virtual count-rates. Each count-rate measurement is correlated with the virtual library and the highest correlated virtual count-rate is found extracting its counter-part virtual flux as the match. Finally, a new intensity factor $\boldsymbol{a}$ is derived from a linear fitting of the measured and virtual count-rates. This new $\boldsymbol{a}$ is directly applied multiplicatively to the virtual flux to produce the unfolded spectrum, this is possible because a simple multiplicative change in the spectrum results in an equal change in the count-rate by definition (c.f. Equation 1). The unfolded spectrum is being used by a Genetic algorithms (GA) as an initial input. The GA is not bound by any strict analytical function offering much more versatility and potentially unfolded spectra that are much closer to reality. The GA process is depicted in the figure below. Each CBR spectrum corresponding to a measurement is randomly perturbed in order to create an initial population of N spectra that are similar but not identical.

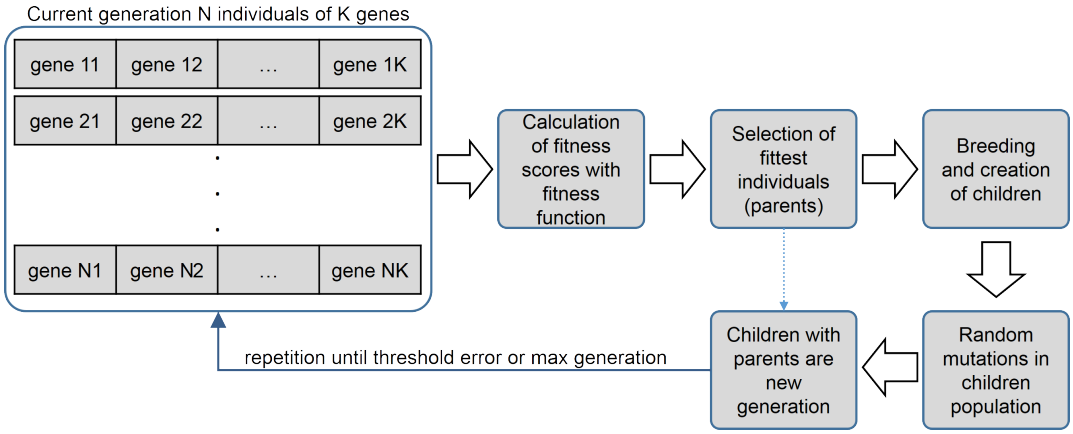

Figure 5: Diagram of the AI part of the GenCORUM process

The flux values at each energy bin are used as the "genes" in the algorithm. Each of the similar spectra is evaluated and scored in terms of how well it reconstructs the measured count-rate. The mean absolute percentage error (MAPE) is used as the fitness (score) function because it is not affected by the absolute values of the counts in the count-rate vector which can often vary by many orders of magnitude.

The process consists of four main steps:

- Fitness evaluation of the population where all the spectra are scored
- Parent selection from the population where the best performing (highest score / lowest error) spectra are selected as "parents"
- Breeding and creation of children population where the selected parents are randomly combined to create again N "children" spectra
- Random mutation of the children spectra where some of the flux values are randomly perturbed

These steps create a new population and they are iteratively repeated, each iteration is dubbed a generation. As generations progress the overall and best performance increases and the overall and lowest error decreases. The differential electron fluxes are calculated in near real-time - as soon as NGRM raw data become available - using a GenCORUM implementation, and is provided in the energy bins listed in Table 4.

Table 4: Characteristics of EDRS-C/NGRM electron differential flux dataset.

Flux Bin	FEDO_ENERGY [MeV]
1	0.18
2	0.27
3	0.40
4	0.60
5	0.88
6	1.30
7	1.93
8	2.90
9	3.40
10	4.00

5 CONSIDERATIONS ON LEVEL-1 DATASETS

A series of evaluation studies of EDSS/NGRM Level 1 flux datasets have been performed [RD 8] taking advantage of the data collected during the transfer from GTO to GEO of EDRS-C.

- For the case of EDSS/NGRM electron fluxes, the results indicate an overall very good agreement with a series of third-party measurements (e.g. Arase/ERG/XEP [RD 7], GSAT/EMU [RD 2]) accounting for the electron energies up to 2.0-2.5 MeV. For higher energies the NGRM electron fluxes start to become, relatively, overestimated by a factor that can reach values of 2 to 3 (cf. Figure 6, Figure 7)
- For the case of SDSS/NGRM proton fluxes, the comparisons performed so far are limited and are based on the measurements during weak Solar Proton Events (SPEs); they indicate, however, that NGRM proton fluxes are underestimated by a factor of the order of two with respect to NOAA GOES-16 data.
- Strong contamination effects in electron flux products are expected during SPEs.
- Weak contamination effects in proton flux products are expected during strong electron flux enhancements of the outer belt.
- The background levels of the 76 MeV proton flux series are elevated.
- Data users are advised to consult the available ephemeris (ECI coordinates) and magnetic coordinate (e.g., L, MLT) variables, derived using the UNILIB library [RD 10] assuming the IGRF model for the internal, and the quiet Olson-Pfitzer 1977 model for the external magnetic field components.

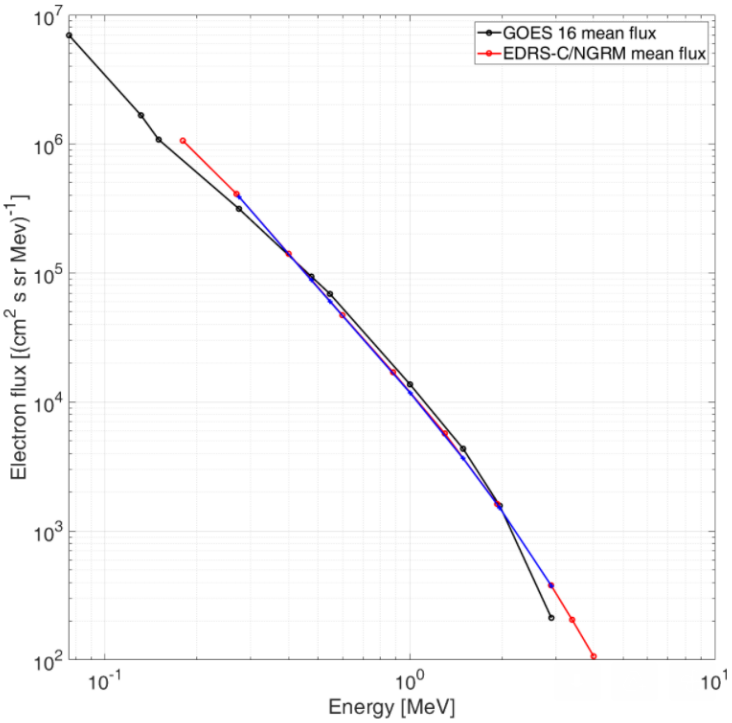

Figure 6: Comparison of mean differential flux spectra between EDRS-C/NGRM and GOES-16 [RD 5] at selected magnetic conjunctions at GEO.

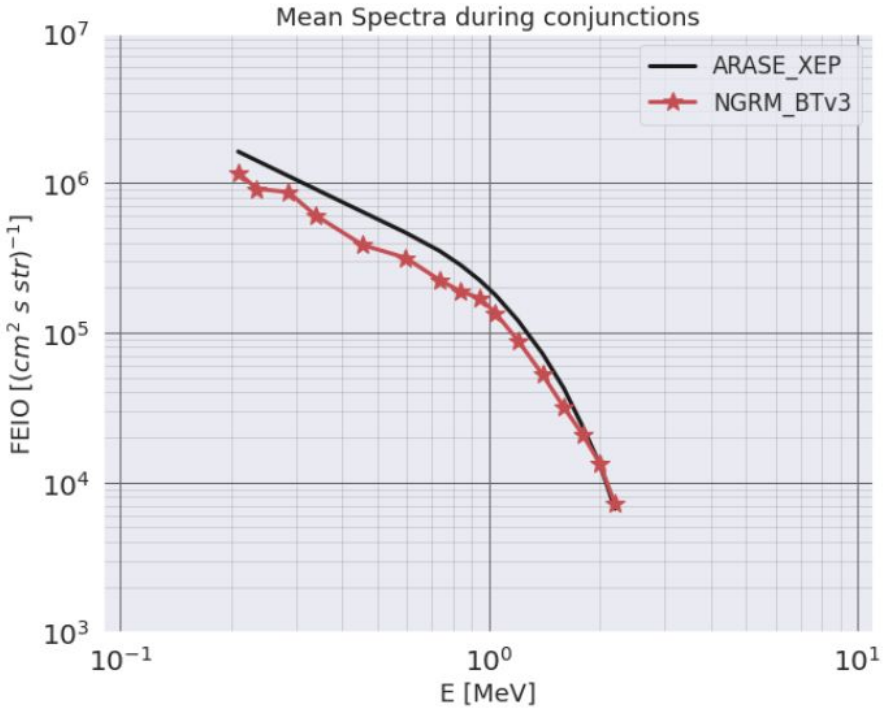

Figure 7: Comparison of the mean integral flux spectra between EDRS-C/NGRM and Arase/XEP [RD 9] at selected magnetic conjunctions during GTO.